Heliyon 6 (2020) e03506

Contents lists available at ScienceDirect

Heliyon

journal homepage: www.cell.com/heliyon

Research article

The effect of DTPA on calcium carbonate scale deposition on copper and aluminium surfaces

K. Palanisamy [a,b], K. Sanjiv Raj [b], S. Bhuvaneswari [a,c], M. Rajasekaran [c,d], V.K. Subramanian [b,e,*]

[a] Dept. of Chemistry, Thiru. A. Govindasamy Govt. Arts College, Tindivanam, 604001, Tamailnadu, India
[b] Dept. of Chemistry, Annamalai University, Annamalainagar, 608 002, Tamilnadu, India
[c] Research and Development Centre, Bharathiar University, Coimbatore, 641046, India
[d] Dept. of Physics, Thiru. A. Govindasamy Govt. Arts College, Tindivanam, 604001, Tamailnadu, India
[e] Dept. of Chemistry, Periyar Govt. Arts College, Cuddalore, 607001, Tamilnadu, India

ARTICLE INFO

Keywords:
Inorganic chemistry
Materials chemistry
DTPA
Water treatment.
Scale
$CaCO_3$
Calcite

ABSTRACT

Calcium carbonate ($CaCO_3$) scale inhibition by Diethylenetriaminepentaacetic acid (DTPA) on copper and aluminium metal surfaces was studied at 60 and 100 °C. The samples were characterized using X-ray diffraction (XRD), Scanning electron microscopy (SEM) and Fourier transform infrared spectroscopy (FTIR). The results revealed a novel pot like morphology for calcite which was resulted from the transformation of dumbbell morphology. The pot like morphology exposed the possibility of hollow structures for other polymorphs and is resulted from the breaking apart of the dumbbell structures at the middle, followed by fluffing of the separated parts.

1. Introduction

Water, the universal solvent due to its abundance, is the most commonly used material for heat transfer applications. It is used in small car radiators to large cooling towers and boilers. Corrosion, scale formation and biological growth are major problems encountered in such heat exchangers [1, 2, 3, 4, 5, 6]. Scale formation is due to the precipitation of insoluble salts, mostly of calcium and magnesium which forms as sludge at high temperatures and gets deposited on the surfaces of equipment leading to reduced heat transfer efficiency and sometimes shutdown of the equipment or even an industrial plant [7].

Different water treatment techniques are adopted for scale inhibition. External treatment such as softening and demineralization removes the major scale causing constituents from the water to a great extend, but makes it more corrosive [7]. This makes internal treatment inevitable, particularly for operations at elevated temperatures and closed systems where the same water is recycled for long period such as in the case of radiators. Internal treatment mainly consists of adding chemicals like coolants which are capable of the scale causing constituents in suspension, thus delaying their deposition [8, 9, 10, 11]. Another major advantage is that they are usually added in the low concentrations (usually 2–10 ppm), thereby having very little impact on the feed water quality [7,12].

Calcium carbonate is found to be one of the major constituents of scale. $CaCO_3$ has three anhydrous crystalline forms; calcite, aragonite and vaterite and three hydrated forms; amorphous calcium carbonate (ACC), monohydrocalcite ($CaCO_3.H_2O$) and ikaite ($CaCO_3.6H_2O$) [13, 14, 15, 16, 17]. Since different polymorphs have different physical properties, polymorphism plays an important role in scale formation [18]. Literature survey indicates that the predominant polymorphic forms of $CaCO_3$ in scale are calcite and aragonite [19, 20, 21] and vaterite is usually not observed.

Among the above different polymorphs decreases in the order of calcite is the most stable, aragonite is meta stable and vaterite is the least stable [22, 23, 24]. The crystallization of $CaCO_3$ starts from unstable ACC, and proceeds to calcite via vaterite and metastable aragonite. This process is governed by many factors such as pH, temperature, presence of additives etc [25, 26, 27, 28, 29, 30, 31, 32, 33]. For example, ACC will transform to calcite via vaterite at low temperatures (<30 °C) and to aragonite via vaterite at higher temperatures (≥40 °C) [34]. Report suggests that grater the vaterite a scale inhibitor can produce, the more efficient it will be [35,37]. But managing the formation of a particular

* Corresponding author.
E-mail address: drvksau@gmail.com (V.K. Subramanian).

https://doi.org/10.1016/j.heliyon.2020.e03506
Received 25 September 2018; Received in revised form 22 November 2019; Accepted 24 February 2020

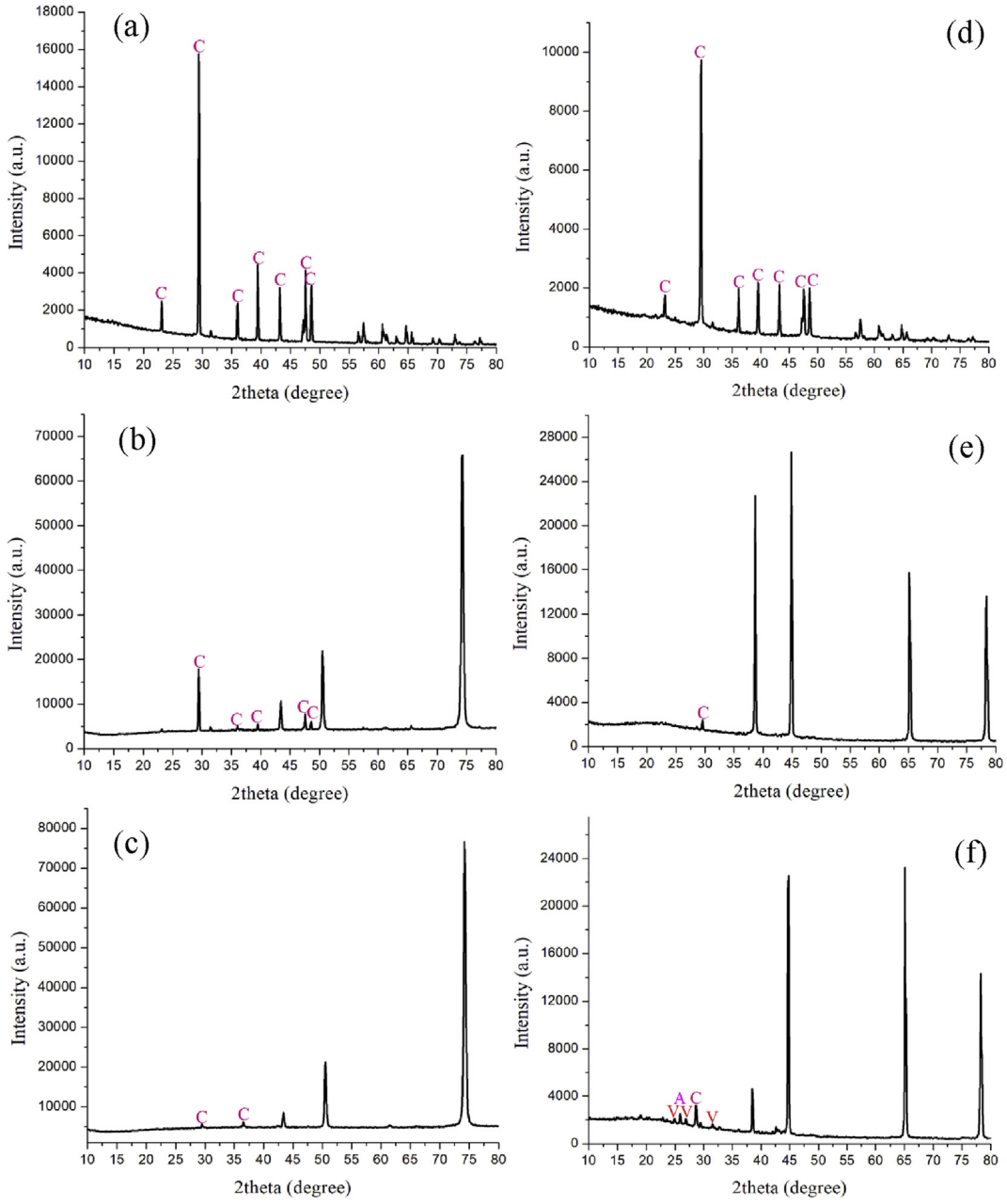

Figure 1. XRD pattern of samples prepared at 60 °C in the presence of DTPA. (a) $CaCO_3$ sludge in presence of copper substrate (b) copper coin-bottom (c) copper coin-suspended (d) $CaCO_3$ sludge in presence of aluminium substrate (e) aluminium coin-bottom (f) aluminium coin-suspended.

polymorph by the controlling the growth of other polymorphs and the ability to predict such reactions still remains as a major challenge [22].

Copper, aluminium, mild steel and alloy steel are the major materials used in the manufacturing of heat transfer equipments. However due to the high thermal conductivity and low corrosion problems, copper and aluminium are extensively used in low and moderate heat exchange (below 100 °C) applications such as radiators and closed loop systems. Report suggests that DTPA [13] has significant ability to affect the polymorphic transformations of $CaCO_3$ and stabilize different polymorphs at different temperatures. However the study limits itself on the synthesis of $CaCO_3$ and does not extend to metal surfaces. This necessitates the study on deposition on different metal surfaces to have the validity of their observations on practical applications. Hence in this study, we have chosen aluminium and copper to understand the mechanism of scale deposition at two different temperatures 60 and 100 °C and the effect of DTPA on $CaCO_3$ scale deposition on these metal surfaces.

2. Experimental sections

Analytical grade $CaCl_2$, Na_2CO_3 and DTPA were obtained from Himedia chemicals, and were used as supplied without further purification. De-mineralized water was used for the preparation of aqueous solutions.

The experimental set up and the procedure followed here is similar to the one detailed by elsewhere [35]. Copper buttons of 0.92×10^{-2} m diameter and 0.75×10^{-3} m thickness and aluminium coins of 0.94×10^{-2} m diameter and 0.94×10^{-3} m thickness were used as substrate. In typical experiment, two buttons were placed in a mixture solution of 100 ml 0.1M calcium chloride and 20 ml 0.1 M DTPA in a beaker (one at the bottom and another in suspension, to study the effect of direct and indirect heating on scale deposition) and heated to 60 °C using a mantle with temperature controller (+/-1 °C) and 150 ml 0.05 M sodium carbonate was introduced drop by drop from a burette 20 min after attaining

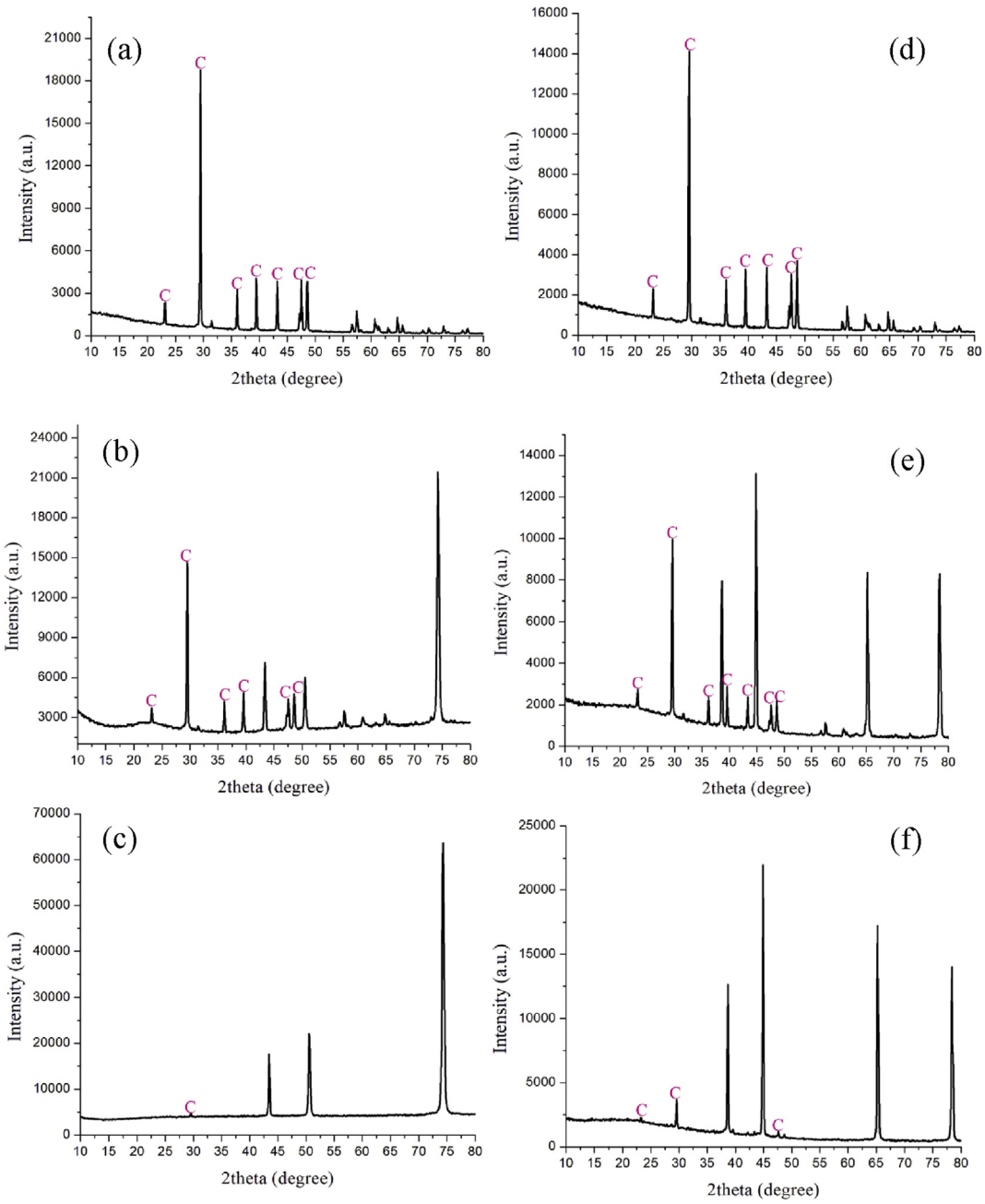

Figure 2. XRD pattern of samples prepared at 100 °C in the presence of DTPA. (a) $CaCO_3$ sludge in presence of copper substrate (b) copper coin-bottom (c) copper coin-suspended (d) $CaCO_3$ sludge in presence of aluminium substrate (e) aluminium coin-bottom (f) aluminium coin-suspended.

the temperature and the whole set up was maintained at same temperature for 10 days. After 10 days, the copper buttons were collected and rinsed with cold distilled water. The precipitate (sludge) from the bottom of the flask was also collected using a Whatman 40 filter paper. All the samples were washed thrice with distilled water and dried at 45 °C in a hot air oven. The experiments were repeated at 100 °C and also using aluminium buttons.

3. Characterization

The samples were characterized by powder XRD method and the morphological studies were done using scanning electron microscope (SEM). The sludge samples were characterized by FT-IR after KBr pelletization. The X-ray diffraction (XRD) pattern were recorded on a Bruker D8 Advanced XRD diffractometer with Cu Kα radiation at λ = 1.5406 Å with the step size of -0.091063. Microscopic morphological images were taken using JEOL JSM-6610 LV, Philips XL30 -ESEM and Hitachi Science systems S–3400N having accelerating voltage of 10–30 kV (in High Vacuum Mode) with Secondary electron Image Resolution: ~ 3.0 nm. The $CaCO_3$ sludge collected from the bottom of the flask was characterized by FTIR in the range 500–4000 cm^{-1} using FT-IR (SHIMADZU).

4. Results and discussions

The XRD pattern of the samples in presence of DTPA at 60 °C is presented in Figure 1 (a-f). Characteristic peaks of calcite were evident at 2θ ~ 29.3° (104), 36.0° (110) 39.4° (113) 43.1° (202) 47.4° (018) 48.5° (116) (JCPDS: 862339) in the sludge sample (Figure 1(a)) in presence of copper. Copper substrate kept at bottom exhibited presence of calcite

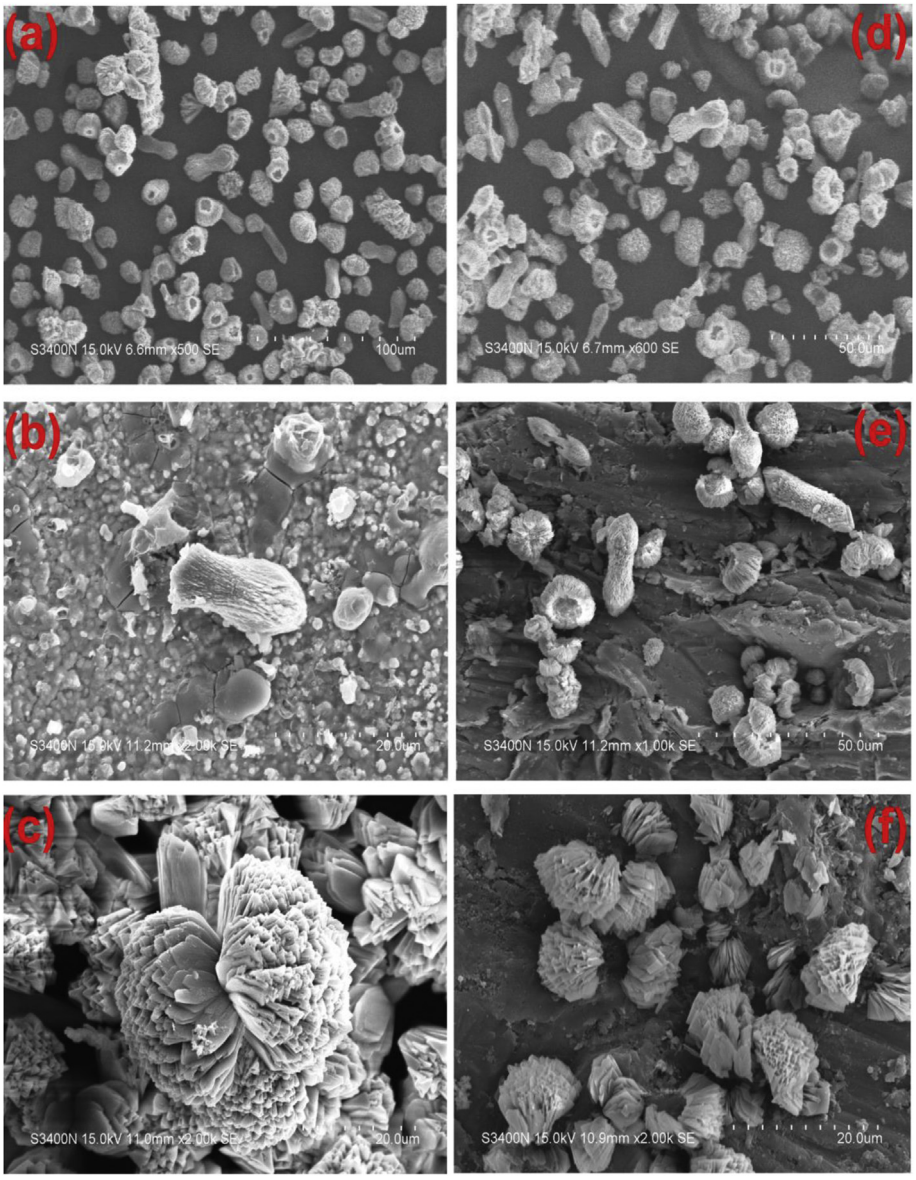

Figure 3. SEM images of samples prepared at 60 °C in the presence of DTPA. (a) $CaCO_3$ sludge in presence of copper substrate (b) copper coin-bottom (c) copper coin-suspended (d) $CaCO_3$ sludge in presence of aluminium substrate (e) aluminium coin-bottom (f) aluminium coin-suspended.

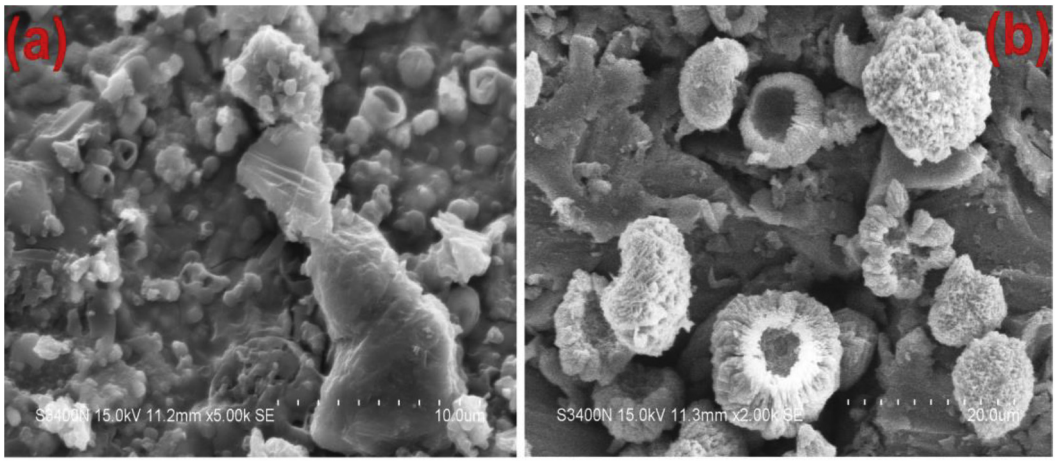

Figure 4. Magnified images of bottoms samples at 60 °C in presence of DTPA (a) copper (b) aluminium.

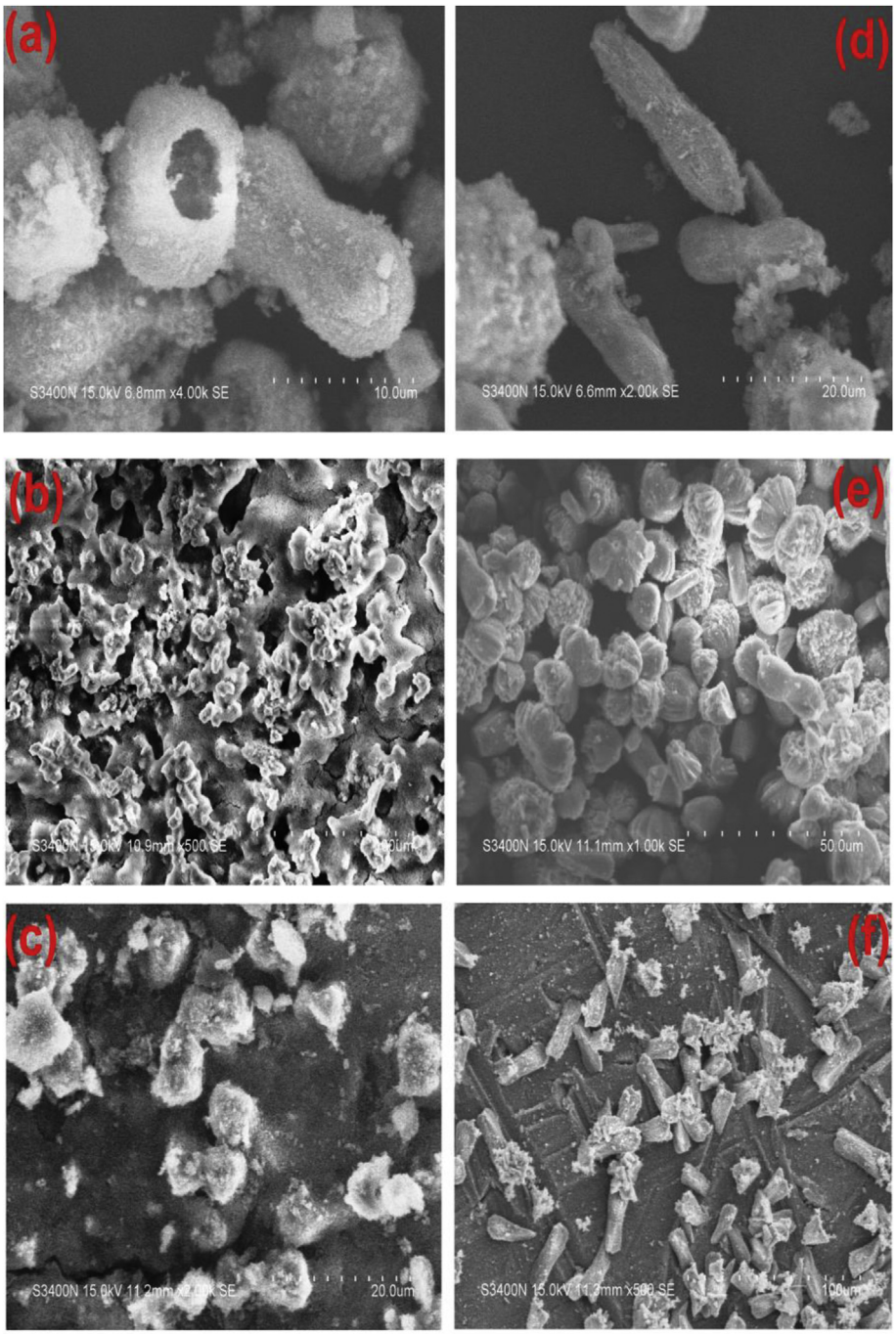

Figure 5. SEM images of samples prepared at 100 °C in the presence of DTPA. (a) $CaCO_3$ sludge in presence of copper substrate (b) copper coin-bottom (c) copper coin-suspended (d) $CaCO_3$ sludge in presence of aluminium substrate (e) aluminium coin-bottom (f) aluminium coin-suspended.

peaks at 2θ ~ 29.4° (104) 36.0° (110) 39.4° (113) 47.6° (018) 48.5° (116) (JCPDS: 721652) (Figure 1(b)). Copper coin kept at suspension also showed presence of calcite alone and contained peaks at 2θ ~ 29.4° (104) 36.0° (110) (JCPDS: 721652) Figure 1(c). Peaks corresponding to other polymorphs were absent.

The XRD pattern of sludge in presence of aluminium at 60 °C showed calcite peaks at 2θ ~ 29.4° (104) 36.0° (110) 39.4° (113) 43.2° (202) (JCPDS: 721652) (Figure 1(d)). Aluminium coin kept at bottom (Figure 1(e)) and in suspension (Figure 1(f)) also contained the characteristic peaks of calcite at 2θ ~ 29.5° (104) and 2θ ~ 28.7° vide (JCPDS: 721650) and (JCPDS: 030569) respectively. The appearance of peaks at 25.8° (111) (JCPDS: 712392) and 24.8° (100) 27.0° (101) 32.7° (102) (JCPDS: 720506) in Figure 1(f) confirmed the presence of aragonite and vaterite in the suspended aluiminium coin.

The XRD pattern of sludge sample in presence of copper (Figure 2 (a)) in presence of DTPA at 100 °C exhibited characteristic peaks at 2θ ~ 29.5° (104) 36.2° (110) 39.5° (113) (JCPDS: 020629) confirming calcite in the sample. Copper button at bottom (Figure 2(b)) also contained calcite and corresponding peaks were observed at 2θ ~ 29.4° (104) 36.0° (110) 39.4° (113) 47.6° (018) 48.5° (116) (JCPDS: 721652). Suspended copper substrate (Figure 2(c)) contained peaks related to calcite alone at 2θ ~ 29.5° (104) (JCPDS: 020629) other peaks of aragonite and vaterite were absent in these samples.

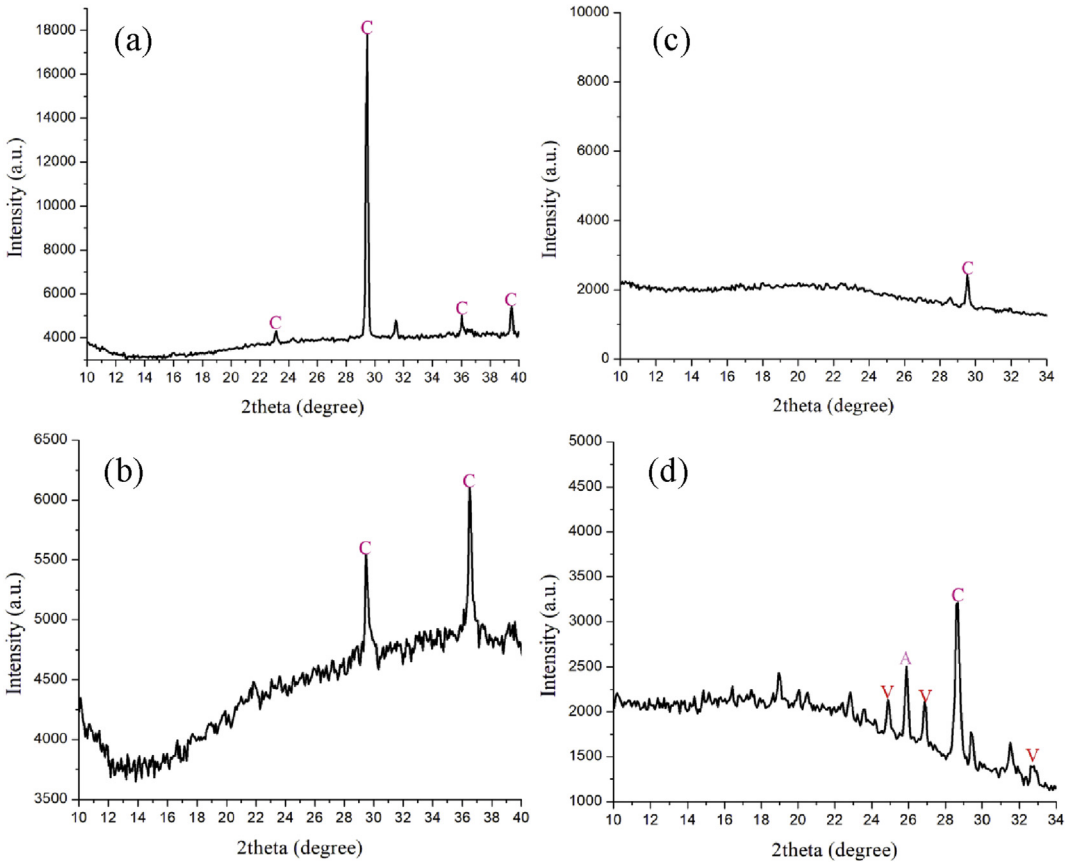

Figure 6. Deconvoluted XRD diffraction pattern of scale deposited substrates at 60 °C; copper bottom (a), copper suspended (b) aluminium bottom(c), aluminium suspended (d).

Figure 2 (d), (e) and (f) depict the XRD pattern of sludge sample in presence of aluminium, aluminium bottom sample and suspended aluminium sample respectively. All these samples contained only characteristic peaks of calcite alone. Peaks at 2θ ~ 29.5° (104) 36.2° (110) 39.5° (113) 43.3° (202) 47.5° (024) 48.6° (116) (JCPDS: 721650) pertaining to calcite were observed in sludge sample.

The XRD pattern of bottom aluminium sample (Figure 2 (e)) showed calcite peaks at 2θ ~ 29.5° (104) 36.2° (110) 39.5° (113) 43.3° (202) 47.5° (024) 48.6° (116) (JCPDS: 020629) while suspended aluminium sample (Figure 2(f)) exhibited calcite peaks at 2θ ~ 29.5° (104) 47.5° (024) (JCPDS: 020629).

Literature survey on the synthesis of $CaCO_3$ in the presence of DTPA revealed that only aragonite were observed at 60 and 80 °C, where as pure calcite was resulted at 100 °C [8]. The probable reason could be the presence of metallic copper in the system. In an earlier study conducted in our lab [38], using ethylene glycol-O,O′-bis(2-aminoethyl)-N,N,N′, N′-tetraacetic acid (EGTA), in the absence of EGTA, aragonite was present in two samples prepared in the copper environment: the sludge at 100◦Cand the suspended copper button at 60 °C. There is no aragonite or vaterite in any of the samples in presence of aluminum. Neverthe-less, the presence of EGTA incorporated considerable amounts of both aragonite and vaterite in the aluminum environment.

The XRD studies revealed a uniform polymorphic composition of calcite in all the samples in presence of DTPA. Only aluminium substrate kept under suspension at 60 °C exhibited presence of aragonite and vaterite along with calcite.

In order to assess whether this uniformity in polymorphic composition remained in morphology also, SEM images of the samples were taken. The SEM images of the samples at 60 °C and 100 °C are presented in (Figure 3 (a-f)) and (Figure 5 (a-f)) respectively. Figure 3 (a) and (d) represents the morphologies of the sludge samples under copper and aluminium substrates respectively. Both the samples exhibited similarity and contained two different types of structures, one resembling peanut and another pot like structures. Both these morphologies could be only that of calcite as XRD results indicated presence of calcite alone in these samples (Figure 1 (a, d)).

The uniqueness of the pot shape is that none of these structures had rim/brim and looked like rim less pots. Shown in (Figure 3 (b)) is the morphology of scale deposited on the bottom copper metal substrate surface at 60 °C. It is obvious from the magnified image (Figure 4 (a)) that very small dumbbell, spherical and the rimless pot like structures of calcite are fused on to the surface of the substrate (Figure 3 (e)). represents the SEM morphology of aluminium substrate kept in the bottom. Scale deposited on the metal surface exhibited both dumbbell shaped and open rimless pot like morphology presented. Nevertheless this sample contained less amount of pot structures and dumbbell/peanut shaped morphology predominated (Figure 4 (b)).

The morphology of scale deposited on the suspended copper and aluminium samples are presented in (Figure 3 (c)) and f respectively. Only dumbbell shaped morphology was observed in the case of copper. However the dumbbell shape was a little different from those observed in sludge or on the bottom samples. Here they resembled more as the unison of two rimless pot structures observed in the earlier samples.

There was some drastic change in the surface texture of the dumbbells. The crystals had shown excellent faceting, indicating crystal growth could be ongoing. However the internal stresses during crystal growth could have caused the fracturing. Another possibility could be erosion leading to rimless pot like structures observed in sludge. The same trend was visible in the case of aluminium substrate. But, the scale

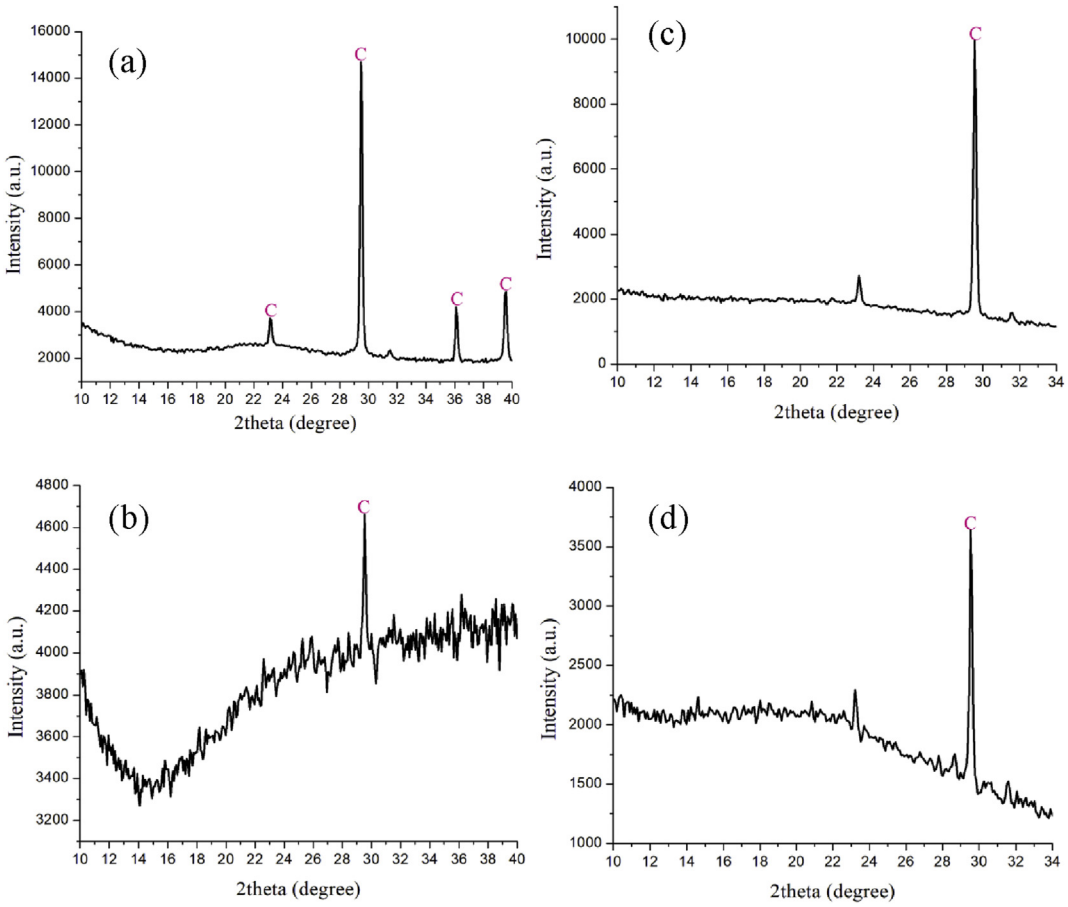

Figure 7. Deconvoluted XRD diffraction pattern of scale deposited substrates at 100 °C; copper bottom (a), copper suspended (b) aluminium bottom (c), aluminium suspended (d).

deposition was rather scanty and the tendency for broken dumbbells was more.

The SEM images of the samples synthesized in the presence of DTPA at 100 °C are presented in Figure 5 (a-f). As in the case of 60 °C, here also the sludge samples in presence of both copper Figure 5 (a) and aluminium Figure 5 (d) contained two morphologies. Even though they resembled much, the dumbbell shape appeared more as peanut shaped and rimless pot like morphology was more spherical in shape. The XRD data indicated that these sludge samples contained only calcite Figure 2 (a, e). The copper coin at the bottom Figure 5(b) exhibited rampant growth of scale in the form of a thick layer over the entire area sparing any bare metal surface.

The morphological examination revealed that there is no much difference in the situation of aluminium substrate (Figure 5 (e)) under similar conditions. It was observed that in both cases larger particles could only contribute in building up the further layers.

Figure 5 (c and f) depicts the SEM images of suspended copper and aluminium substrates respectively in the presence of DTPA. The suspended copper coin contained less scale deposition and the morphology resembled the pot like structures observed in sludge samples. In the case of aluminium coin (Figure 4 (f)), the morphology more resembled the dumbbell structures but they were showing less recession at the centre, making them resemble thick rods. The suspended substrate contained considerably less severe scale deposition. Earlier reports on the morphology of $CaCO_3$ in the presence of DTPA have shown needle/thorn-like aragonite at 60 °C [13]. They showed tendency to agglomerate with increase in temperature. At 80 °C the sample showed agglomerated thorns resulting into a spherolite/datura pod structure, mostly two units joined together. A marginal change in the morphology with a remarkable change in the crystal structure was observed at 100 °C. The morphology became dumbbell in shape. Hence this dumbbell morphology could be attributed to the characteristic structure in presence of DTPA.

Due to the very high intensity of the XRD peaks of both copper and aluminium metals, the intensities of the different polymorphs of $CaCO_3$ (particularly aragonite and vaterite, due to their comparatively low intensities and percentage composition in the sample) are subdued. However, most of the metal peaks are appeared beyond $2\theta \sim 40^{\circ}$ and most of the 100 % peaks of all the polymorphs of $CaCO_3$ are observed below this 2θ value. Hence in order to ascertain the interpretations made in XRD analysis are correct and no vaterite or aragonite is present in the cases where calcite alone is observed, the XRD pattern of the metal substrates at 60 and 100 °C were deconvoluted to have the $CaCO_3$ peaks seen distinct from the metal peaks and are presented in Figures 6 and 7 respectively.

The deconvoluted XRD pattern clearly indicated presence of only calcite in bottom and suspended copper substrates at both 60 and 100 °C and in bottom aluminium substrate at 60 °C and both bottom and suspended aluminium substrates at 100 °C. Aragonite and vaterite peaks were present in suspended aluminium substrates.

The polymorphic composition of the sludge samples were further ascertained by FTIR and compared with standard values [39]. The FTIR spectra of sludge in presence of copper and aluminium substrates at 60 and 100 °C are presented in (Figure 8 (a-d)). The bands corresponding to calcite alone were observed at ~711 (ν_4), ~1085 (ν_1) and ~1435 (ν_3) cm^{-1} and none of the samples contained either aragonite or vaterite. As

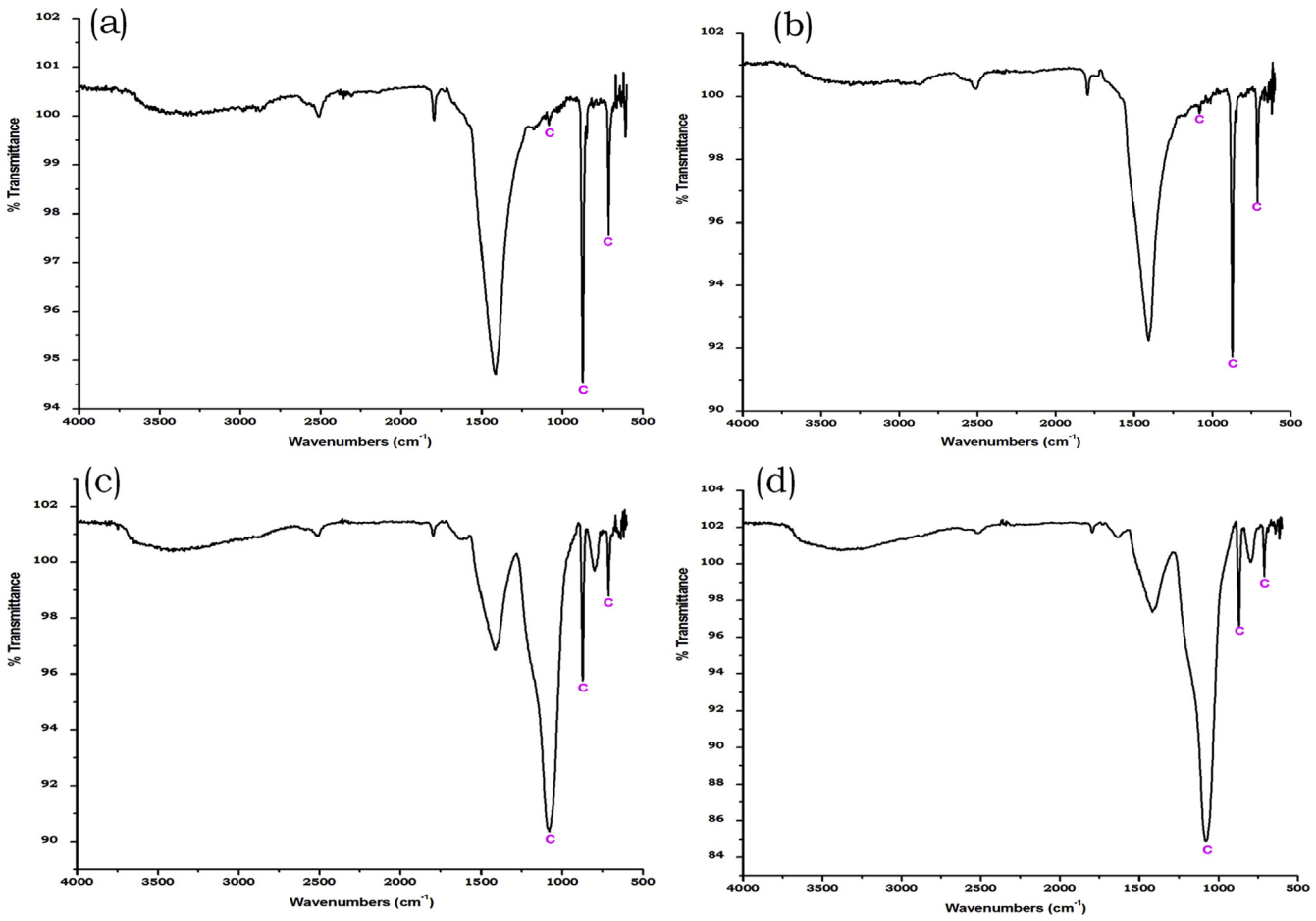

Figure 8. FTIR spectra of $CaCO_3$ sludge in the presence of DTPA and a) copper at 60 °C (b) aluminium at 60 °C (c) copper at 100 °C (d) aluminium at 100 °C.

in the case of XRD, aragonite (~700 cm^{-1}) and vaterite (~745 cm^{-1}) bands have less intensities when compared to calcite. In order to reconfirm that aragonite bands are not present, the FTIR were deconvoluted and presented in Figure 9. Absence of peaks at ~ 700 and 745 cm^{-1} in all the Figures reconfirmed that the sludge sample contained only calcite.

5. Mechanism

It could be inferred from the above discussions that, during the crystal growth the morphology of the crystallites are influenced by presence of DTPA. In the absence of DTPA (blank), a binary mixture of calcite and aragonite were observed in copper suspended sample at 60 °C. All other samples contained only calcite. All the samples invariably exhibited rhombohedral structures attributing to calcite. Only the suspended copper substrate contained some fibrous needle like morphology corresponding to aragonite. On increasing the temperature from 60 to 100 °C, the presence of DTPA resulted only calcite in sludge.

In the case of DTPA though the rim less pot like morphology appears to be different from the dumbbell, a close observation of the SEM images elucidate that the former pop up from the latter. The size of the dumbbell morphology is found to be ~25 μm and the diameter of the pot structures are about 10–15 μm.

The mechanism of $CaCO_3$ scale deposition on copper and aluminium in the presence of DPTA could be explained as follows. A certain minimum concentration of scale inhibitor is necessary to prevent scale formation efficiently which is called minimum inhibitor concentration (MIC) [20]. When the concentration of inhibitor is less than MIC, the active growth sites to be controlled become more and the growth of calcite crystal nucleus is correspondingly enhanced. But the DTPA can interact with metal and form complex. This is more evident in the case of copper where the solution turned slight bluish after the experiments. Aluminium being less susceptible to complex formation is less affected. This reduces the effective availability of the DTPA in the case of copper than aluminium.

Detailed examination of the morphologies revealed that the pot like structures is resulted from the breaking apart of the dumbbell structures at the middle, followed by fluffing of the separated parts. The pictorial representation of transformation of dumbbell like morphology to the pot like structures is given in Figure 10.

Even though there are some minor morphological differences in the shape of dumbbells in the presence of copper and aluminium, they are comparable and the above transformation mechanism is found to be applicable for both substrates.

In our earlier studies with EDTA and NTA we observed significant contribution of the substrates on the stabilization of different polymorphic forms of $CaCO_3$ [35,36,37]. Here, in the presence of DTPA aluminium substrate exhibited tendency to stabilize vaterite, but at lower temperature and only on the suspended substrate. This indicates that the vaterite to calcite has been stalled only in the case of suspended substrate where the heating was not direct.

6. Conclusion

The present study elucidate that in the presence of DTPA, the polymorphic composition of scale did not undergo significant transformation with time and is uniform with copper and aluminium substrates.

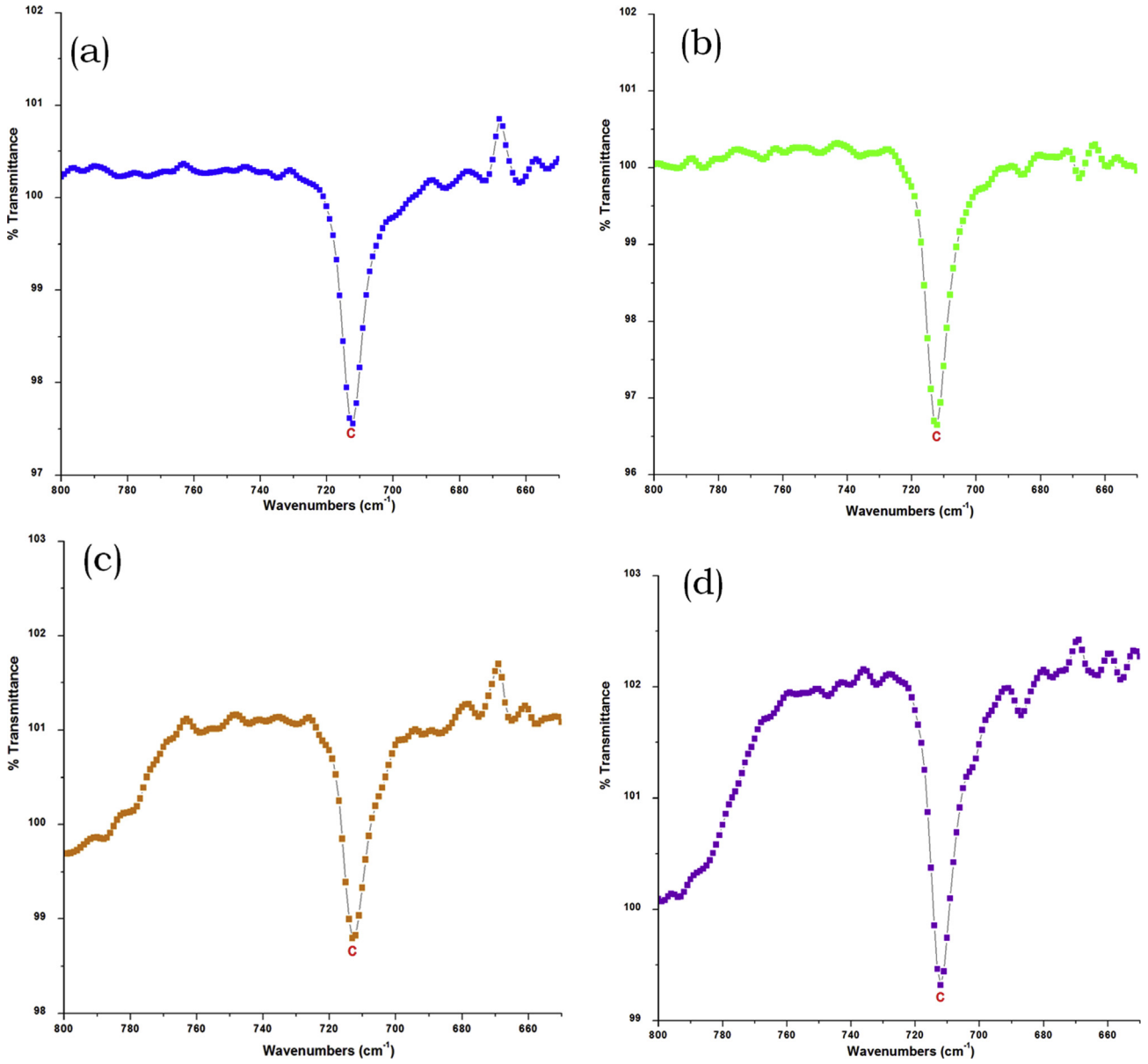

Figure 9. Deconvoluted FTIR of $CaCO_3$ sludge samples synthesized in the presence of DTPA and (a) copper at 60 °C (b) aluminium at 60 °C (c) copper at 100 °C (d) aluminium at 100 °C.

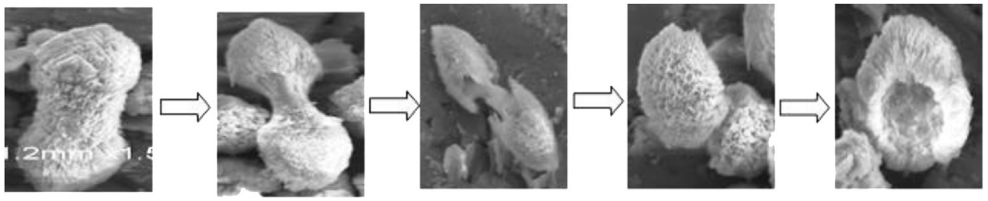

Figure 10. Mechanism of transformation of dumbbell morphology to rimless pot like morphology in the presence of DTPA.

Secondly, the scale deposition was scanty and did not change much with the mode of heating. This is very important as in case of cooling towers where heating does not take place and the hot water is only allowed to circulate through pipes and allowed to cool by natural or artificial draft by sprinkling from towers, DTPA can effectively control scale formation. Thirdly the pot like morphology which is the transformation of the dumbbell morphology revealed that the dumbbell structures are not solid, but hollow masses. This is a novel and important observation as further studies can be carried out on scales with three dimensional structures that can be ruptured which can result into unstable deposition.

Declarations

Author contribution statement

VK Subramanian: Conceived and designed the experiments.

K Palanisamy: Performed the experiments; Analyzed and interpreted the data.

Bhuvaneswari S: Analyzed and interpreted the data; Contributed reagents, materials, analysis tools or data.

Rajasekaran M: Analyzed and interpreted the data; Wrote the paper.

K Sanjiv Raj: Analyzed and interpreted the data.

Funding statement

This research did not receive any specific grant from funding agencies in the public, commercial, or not-for-profit sectors.

Competing interest statement

The authors declare no conflict of interest.

Additional information

No additional information is available for this paper.

References

[1] A.P. Watkinson, O. Martinez, Scaling of heat exchanger tubes by calcium carbonate, J. Heat Tran. 97 (4) (1975) 504–508.
[2] S.H. Chan, K.F. Ghassemi, Analytical modeling of calcium carbonate deposition for laminar falling films and turbulent flow in annuli: Part II- multispecies model, J. Heat Tran. 113 (3) (1991) 741–746.
[3] S.H. Chan, K.F. Ghassemi, Analytical modeling of calcium carbonate deposition for laminar falling films and turbulent flow in annuli: Part I - formulation and single -species model, J. Heat Tran. 113 (3) (1991) 735–740.
[4] S.H. Najibi, H. Müller-Steinhagen, M. Jamiaiahmadi, Calcium carbonate scale formation during subcooled flow boiling, J. Heat Tran. 119 (4) (1997) 767–775.
[5] S.M. Zubair, A.K. Sheikh, M.O. Budair, M.U. Haq, A. Quddus, O.A. Ashiru, Statistical aspects of $CaCO_3$ fouling in AISI 316 stainless – steel tubes, J. Heat Tran. 119 (1997) 581–588.
[6] Z. Amjad, P.G. Koutsoukos, Evaluation of maleic acid based polymers as scale inhibitors and dispersants for industrial water applications, Desalination 335 (2014) 55–63.
[7] S.P. Gopi, V.K. Subramanian, Anomalous transformation of calcite to vaterite: significance of HEDP on crystallization behavior and polymorphism at elevated temperatures, Indian J. Chem. 52 (2013) 342–349.
[8] Y.P. Lin, P.C. Singer, Inhibition of calcite crystal growth by polyphosphates, Water Res. 39 (2005) 4835–4843.
[9] K.A. Anezi, D.J. Johnson, N. Hilal, An atomic force microscope study of calcium carbonate adhesion to desalination process equipment: effect of anti-scale Agent, Desalination 220 (2008) 359–370.
[10] K. Naka, Y. Chujo, Control of crystal nucleation and growth of calcium carbonate by synthetic substrates, Chem. Mater. 13 (2001) 3245–3259.
[11] L. Pach, S. Duncan, R. Roy, S. Komarneni, Morphological control of precipitated calcium, J. Mater. Sci. 31 (1996) 6565–6569.
[12] Z. Amjad, Precipitation of calcium carbonate in aqueous systems, Tenside Surfactants Deterg. 36 (1999) 162–167.
[13] S.P. Gopi, V.K. Subramanian, K. Palanisamy, Aragonite–calcite–vaterite: a temperature influenced sequential polymorphic transformation of $CaCO_3$ in the presence of DTPA, Mater. Res. Bull. 48 (2013) 1906–1912.
[14] A. Antony, J.H. Low, S. Gray, A.E. Childress, P. Le-Clech, G. Leslie, scale formation and control in high pressure membrane water treatment systems: a review, J. Membr. Sci. 383 (2011) 1–16.
[15] H. Tang, J. Yu, X. Zhao, Controlled synthesis of crystalline calcium carbonate aggregates with unusual morphologies involving the phase transformation from amorphous calcium carbonate, Mater. Res. Bull. 44 (2009) 831–835.
[16] L. Addadi, S. Raz, S. Weiner, Taking advantage of disorder: amorphous calcium carbonate and its roles in biomineralization, Adv. Mater. 15 (2003) 959–970.
[17] S.P. Gopi, K. Palanisamy, V.K. Subramanian, Effect of NTA and temperature on crystal growth and phase transformations of $CaCO_3$, Desalin. Water Treat. 54 (2014) 1–9.
[18] S.P. Gopi, V.K. Subramanian, Polymorphism in $CaCO_3$-Effect of Temperature under the Influence of EDTA (di sodium salt), Desalination 297 (2012) 38–47.
[19] J.R. Hart, Ethylenediaminetetraacetic acid and related 421 chelating agents. InUllmann's Encyclopedia of Industrial Chemistry, Wiley-VCH, Weinheim, Germany, 2000, p. 422.
[20] G.C. Zhang, J.J. Ge, M.Q. Sun, B.L. Pan, T. Mao, Z.Z. Song, Investigation of scale inhibition mechanisms based on the effect of scale inhibitor on calcium carbonate crystal forms, Sci. China B Chem. 50 (2007) 114–120.
[21] Y. Tang, W. Yang, X. Yin, Y. Liu, P. Yin, J. Wang, Investigation of $CaCO_3$ scale inhibition by PAA, ATMP and PAPEMP, Desalination 228 (2008) 55–60.
[22] S.P. Gopi, V.K. Subramanian, K. Palanisamy, Synergistic effect of EDTA and HEDP on the crystal growth, polymorphism, and morphology of $CaCO_3$, Ind. Eng. Chem. Res. 54 (2015) 3618–3625.
[23] S. Timo, T. Wolfgang, Versatile wet-chemical synthesis of non-agglomerated $CaCO_3$ vaterite nanoparticles, Chem. Commun. 47 (2011) 5208–5210.
[24] Q.S. Wu, D.M. Sun, H.J. Liu, Y.P. Ding, Abnormal polymorph conversion of calcium carbonate and nano-self-assembly of vaterite by A supported liquid membrane system, Cryst. Growth Des. 4 (2004) 717–720.
[25] F.A. Setta, A. Neville, Efficiency assessment of inhibitors on $CaCO_3$ precipitation kinetics in the bulk and deposition on A stainless steel surface (316 L), Desalination 281 (2011) 340–347.
[26] Z. Hu, Y. Deng, Supersaturation control in aragonite synthesis using sparingly soluble calcium sulfate as reactants, J. Colloid Interface Sci. 266 (2003) 359–365.
[27] J. Chen, L. Xiang, Controllable synthesis of calcium carbonate polymorphs at different temperatures, Powder Technol. 189 (2009) 64–69.
[28] K. Al-Anezi, D.J. Johnson, N. Hilal, An atomic force microscope study of calcium carbonate adhesion to desalination process equipment: effect of anti-scale Agent, Desalination 220 (2008) 359–370.
[29] A.E. Al-Rawajfeh, H. Glade, J. Ulrich, Scaling in multiple-effect distillers: the role of CO_2 release, Desalination 182 (2005) 209–219.
[30] A.M. Shams-el-din, R.A. Mohammed, Brine and scale chemistry in MSF distillers, Desalination 99 (1994) 73–111.
[31] D. Hasson, Development of the electrochemical scale removal technique for desalination applications, Desalination 230 (2008) 329–342.
[32] G. Atkinson, M. Mecik, The chemistry of scale prediction, J. Petrol. Sci. Eng. 17 (1997) 113–121.
[33] M.B. Amor, Influence of water hardness, substrate nature and temperature on heterogeneous calcium carbonate nucleation, Desalination 166 (2004) 79–84.
[34] J.D. Rodriguez-Blanco, S. Shaw, L.G. Benning, The kinetics and mechanisms of amorphous calcium carbonate (ACC) crystallization to calcite, via vaterite, Nanoscale 3 (2011) 265–271.
[35] K. Palanisamy, V.K. Subramanian, $CaCO_3$ scale deposition on copper metal surface; effect of morphology, size and area of contact under the influence of EDTA, Powder Technol. 294 (2016) 221–225.
[36] K. Palanisamy, V.K. Subramanian, An investigation into the effect of NTA on scale deposition from $CaCO_3$ sludge on copper metal surface, Biointerface Res. Appl. Chem. 6 (2016) 1166–1171.
[37] K. Palanisamy, K. Sanjiv Raj, S. Bhuvaneswari, V.K. Subramanian, A novel phenomenon of effect of metal on calcium carbonate scale, morphology, polymorphism and its deposition, Mater. Res. Innovat. (2016) 1–10.
[38] K. Palanisamy, K. Sanjiv Raj, M. Nirmala Devi, V.K. Subramanian, Effect of EGTA and metal induced polymorphic selectivity of calcium carbonate scale on copper and aluminum, Materials Discovery 4 (2016) 8–17.
[39] N.V. Vagenas, A. Gatsouli, C.G. Kontoyannis, Quantitative analysis of synthetic calcium carbonate polymorphs using FT-IR spectroscopy, Talanta 59 (2003) 831–836.